Renewable Empower Distribution of the World

Article *in* Journal of Environmental Accounting and Management · April 2019

DOI: 10.5890/JEAM.2019.03.002

2 authors:

Dong Joo Lee
Gwangju Institute of Science and Technology
10 PUBLICATIONS **18** CITATIONS
SEE PROFILE

Mark Brown
University of Florida
202 PUBLICATIONS **9,236** CITATIONS
SEE PROFILE

Journal of Environmental Accounting and Management

Journal homepage: https://lhscientificpublishing.com/Journals/JEAM-Default.aspx

Renewable Empower Distribution of the World

Dong Joo Lee, Mark T. Brown†

Department of Environmental Engineering Sciences, University of Florida, USA

Submission Info

Communicated by Zhifeng Yang
Received 17 April 2018
Accepted 22 October 2018
Available online 1 April 2019

Keywords

Emergy
Global Empower
GIS
Renewable energy

Abstract

Large spatial scale emergy analysis can benefit from the latest spatial datasets that are the result of satellite-based models. This study utilized global spatial datasets developed by NASA and others to perform a global scale emergy analysis, producing global coverages of renewable energy sources leading to global coverages of empower for the renewable inputs to the geobiosphere. Total Aerial Empower Intensity (AEI) was computed for each 1 arc degree cell of Earth by taking the maximum value between the sum of the solar, tidal and geothermal inputs and the largest of the secondary inputs (wind, rain, runoff) for each cell.

An important issue related to spatial emergy analysis was highlighted during this study. Previous methods of computing Unit Emergy Values (UEVs) (or transformities) for secondary and tertiary renewable flows (wind, precipitation, and chemical and geopotential exergy of runoff) relied on global average data. With these spatially explicit global data, new UEVs were computed that rely on spatially explicit fluxes of wind, rainfall, elevation, and modeled total dissolved solids data. Using these data and GIS it is possible to compute regional UEVs for chemical and geopotential exergy of runoff.

Finally, we identify an interesting and well-known phenomenon in spatial analysis known as the Modifiable Areal Unit Problem (MAUP) and explore how it impacts spatial emergy evaluations. The MAUP results from spatial aggregation and scale of analysis and ultimately results in statistical bias when summary statistics are computed from spatial data. Our recommendation is first to be aware of MAUP when dealing with analysis of spatial data and second, when aggregating data over regions it is best to minimize subdivisions. Considering this outcome we suggest that evaluations that employ the max emergy algebra and GIS be done at the coarse scale of the regional boundary, rather than on a cell by cell basis.

1 Introduction

With the increased availability of spatial data at the global scale it has become apparent that emergy evaluation of large-scale systems like nations and Earth biomes can benefit from these global data sets. Until now, emergy evaluation of nations and biomes were based on scalar data (some renewable inputs obtained from spatial data aggregated to single values for each country or biome). Sweeney et al. (2006) evaluated renewable inputs using spatial data sets aggregated to single value for countries. Brandt-Williams and Brown (2011) used spatial data

†Corresponding author.
Email address: mtb@ufl.edu

ISSN 2325-6192, eISSN 2325-6206/$-see front materials
DOI:10.5890/JEAM.2019.03.002

Table 1 Sources and specification for spatial datasets.

Data	Solar	Resolution	1 arc degree
URL	https://eosweb.larc.nasa.gov/cgi-bin/sse/global.cgi?email=skip@larc.nasa.gov		
Data	Geothermal [a]	Resolution	2 arc degree
URL	http://onlinelibrary.wiley.com/doi/10.1002/ggge.20271/abstract		
Data	Tidal [b]	Resolution	10 arc min
URL	http://www.nature.com/nature/journal/v405/n6788/abs/405775a0.html?foxtrotcallback=true		
Data	Wind speed		1 arc degree
URL	https://eosweb.larc.nasa.gov/cgi-bin/sse/global.cgi?email=skip@larc.nasa.gov		
Data	Surface roughness	Resolution	500 m
URL	https://modis.gsfc.nasa.gov/data/dataprod/mod12.php		
Data	Land Precipitation	Resolution	30 arc sec
URL	http://worldclim.org/version2		
Data	AET [c]	Resolution	30 arc sec
URL	http://www.cgiar-csi.org/data/global-high-resolution-soil-water-balance		
Data	Flow Accumulation	Resolution	Polyline
URL	http://www.sciencedirect.com/science/article/pii/S0304380014001288		
Data	DEM	Resolution	3 arc sec
URL	http://viewfinderpanoramas.org/dem3.html		

[a.] Surface heat flow data was downloaded from the supplemental material (Davies, 2013).

[b.] Tidal energy dissipation data was acquired directly from the authors (Egbert and Ray, 2000, 2001).

[c.] Actual Evapotranspiration.

sets to evaluate the ecosystem service value of Earth biomes. In both studies, data were from various sources and of variable quality and scale. Recent advances in geospatial data availability make more detailed evaluation of the renewable resource base for countries and earth biomes possible. This study has developed a GIS raster coverages of global renewable empower distribution using recent spatial data from satellite-based models. These coverages can be used to evaluate the biotic natural capital (BNC) and ecosystem services (ES) of Earth biomes and the renewable empower of countries or any desired spatial system.

2 Methods

2.1 Acquiring available energy (exergy) data

There are various datasets available for global renewable energy distribution. Most datasets are the result of models based on satellite measurements and have resolution finer than or equal to 1 arc degree cell size. Based partly on the resolution of available data and partly on limitations of computational power, all datasets were aggregated into 1 arc degree resolution. Table 1 shows a list of datasets that were used in this study.

2.1.1 Global primary renewable exergy: the global tripartite

The global tripartite is composed of the primary renewable sources driving the geobiosphere, solar, geothermal, and tidal exergy.

Solar exergy - Data from the Surface meteorology and Solar Energy (SSE) dataset, (a part of NASA's Prediction of Worldwide Energy Resource (POWER) Project) were used to develop the empower coverage of solar radiation. The NASA dataset provides solar energy data derived from satellite observation in forms of global horizontal radiation, diffuse radiation, direct normal radiation, and latitude tilt radiation with a 22 year (July

Table 2 The surface roughness exponent for various vegetation types (Chandler et al., 2005)

IGBP Type	Vegetation Type	Surface Roughness Exponent
2, 13	Broadleaf evergreen trees	0.47
1, 5	Needleleaf evergreen trees	0.38
3	Needleleaf deciduous tree	0.39
4, 8, 9, 11	Savanna	0.41
6, 7, 10, 12, 16, 18	Perennial Groundcover	0.27
14	Crop	0.32
15	Rough glacial snow/ice	0.31
	Open water	0.10

1983 – June 2005) annual and monthly average solar radiation data layers on a 1 arc degree resolution. We used annual average horizontal radiation data derived from the 22-year data set to yield average annual solar exergy absorbed, equal to 3.73 E24 J yr^{-1} (Brown et al., 2016).

Geothermal exergy - In 2013, Davies (2013) developed the global surface heat flow map based on 38,374 global heat flow measurement points yielding an estimate of total earth surface heat flux from the interior of 44 TW. Surface heat flow energy was converted to exergy using an average Carnot efficiency of 69% (based on a weighted average of Carnot efficiencies for crustal, mantel and core sources). And then normalized to global geothermal exergy of 9.52 E20 J yr^{-1} (Brown et al., 2016).

Tidal exergy - The tidal energy dissipated on earth was calculated by using a model based on satellite altimeter data from Topex/Poseidon (Egbert and Ray, 2001, 2000). Since not all tide can be measured or modeled accurately, we used data for the M2 tide, which is about 75% of global tide energy and the one that can be modeled most accurately. These data were then normalized by assuming that the M2 tide was reflective of the entire tidal exergy absorbed (1.17 E20 J yr^{-1}) (Brown et al., 2016).

2.1.2 Global secondary renewable exergy

Available Energy of Wind - Brown and Ulgiati (2016) developed a procedure to compute the available energy of wind that is absorbed on lands and ocean by using the difference between wind speed at the surface (0 mps) and the average geostrophic wind speed. To calculate the geostrophic wind velocity, the measured wind speed and the surface roughness exponent are required (Eq.1). Measured wind speed was obtained from NASA's Surface meteorology and Solar Energy (SSE) dataset of annual average 50 meter wind speed based on the NASA Version 1 Goddard Earth Observing System (GEOS-1) satellite on a one arc degree resolution. Surface roughness data from Chandler et al. (2005) were assigned to NASA's Moderate Resolution Imaging Spectroradiometer (MODIS) land cover data as shown in Table 2. Using the 50 m reference velocity and the surface roughness exponent, the geostrophic wind velocity was computed according to Equation 1. Then using the geostrophic wind velocity, the available energy of wind that is absorbed within each cell of the coverage was computed using Equation 2.

$$V = V_{ref} * (Z/Zref)^{\alpha} \tag{1}$$

where, V_{ref} = Reference velocity from NASA's wind speed coverage, Z_{ref} = Reference height = 50 m, Z = height for geostrophic velocity V = 1,000 m, α = surface roughness exponent (determined by land cover data from MODIS).

$$E_{wind} = 1/2\rho * KGN * V^3 * A * T \tag{2}$$

where, ρ = Air density = 1.23 kg m^{-3}, KGN = geostrophic drag coefficient 1.26 E-03 (over sea) and 1.64 E-03 (over land) (Garratt, 1992), A = area of each cell, T = 3.15 E7 s y^{-1}, V = geostrophic wind velocity.

Chemical Potential Energy of Rain and AET – Average annual precipitation data were obtained from WorldClim version 2 at 10 arc minute resolution (Fick and Hijmans, 2017). Total precipitation was split into two com-

ponent pathways. The first was rainfall used by vegetation, equal to evapotranspiration (AET); and the second was surface runoff, equal to the difference between total rainfall and AET. Actual evapotranspiration (AET) data were obtained from Global High-Resolution Soil-Water Balance dataset produced by the Consultative Group on International Agricultural Research, Consortium for Spatial Information (CGIAR-CSI). It provides 10 arc minute resolution hydrological raster data of average annual AET from 1950 to 2000 (Trabucco and Zomer, 2010).

The potential energy in rainfall is its chemical potential energy, which is the energy that can be released during a chemical reaction which can be translated as the partial molar Gibbs free energy (Cook and Dickerson, 1995; Job and Herrmann, 2006). Gibbs free energy in the fresh water in rainfall is computed using the concentration of fresh water in rain compared to sea water. Since average total dissolved solids (TDS) in rainfall is 10 ppm, the concentration of freshwater is 999,990 ppm and that of seawater is 35 ppt TDS so the concentration of freshwater is 965,000 ppm. Gibbs energy is computed using the concentration of fresh water as follows:

$$\Delta G_d = \frac{RT}{w} \ln\left(\frac{999,990}{965,000}\right) = 4.72 J g^{-1}. \tag{3}$$

The chemical potential energy of water that is used by terrestrial vegetation within each cell is the water that is evapotranspired, taken from the AET dataset, while the chemical potential of rain over the ocean uses the entire rainfall. Both are multiplied by the Gibb's free energy, of water using Equation 4 to obtain the chemical potential of freshwater used in each cell of the global coverage.

$$E_{chem} = m * G \tag{4}$$

where, E_{chem} = Chemical potential energy, m = Mass of water, G = Gibbs free energy of rain (from Eq.3).

Chemical Potential energy in runoff – Runoff was computed for each 10 arc minute cell as the difference between rainfall and AET. Surface runoff has both chemical potential and geopotential. Chemical potential of runoff was computed based on Equations 3 and 4. The mass of water was computed using a 250 m resolution digital elevation model (DEM) based on the NASA's 2000 Shuttle Radar Topography Mission (SRTM) and the flow accumulation function in ArcGIS. To compute the Gibbs energy in each cell of the accumulated runoff, the concentration of fresh water in each cell was modeled assuming that cells in the upper reaches had total dissolved solids (TDS) equal to 400 ppm and TDS of the runoff at the ocean interface of 100 ppm (based on the Amazon river: (Gibbs, 1967). TDS in each cell along a flow path was normalized across each catchment based on catchment length so that the longest flow path varied from 400 ppm in the headwaters to 100 ppm TDS at its ocean outfall. In this way a flow path of half this length would have a salinity of 250 ppm TDS at the ocean; likewise a flow path 1/10th of the longest would have a TDS of 370 ppm TDS. Once salinity was assigned to each cell, the Gibbs free energy of fresh water "used" in each cell was computed using Eq. 3 and based on the difference between the cell and its downstream neighbor. Total chemical energy of the flow path was the sum of chemical potential used in each cell.

Geopotential energy in runoff - To compute the geopotential energy of runoff, the quantity of runoff in each cell as well as the elevation was required. The quantity of runoff in each cell was computed as the difference between rainfall and AET and the flow accumulation function in ArcGIS. Using the DEM from above, the height difference between each cell in a flow path and its neighboring cell was obtained and then using Eq.5 the geopotential was computed for each cell of the flow path. The geopotential energy "used" in each cell along a flow path was summed to obtain the total geopotential energy of the flow path.

$$E_{geopotential} = m * g * h \tag{5}$$

where m = Mass of water accumulated, g = Gravity (9.8 m/s^2), h = Elevation difference in refence to neighboring cell.

2.2 Unit emergy values (UEVs)

Unit emergy values used in this study are based on the 12.0 E24 sej yr^{-1} global emergy baseline (Brown et al., 2016) as follows.

2.2.1 Tripartite

The solar equivalence ratios (SERs)[a] for the tripartite were computed by Brown et al. (2016). Solar exergy absorbed on earth has an SER of 1 seJ J^{-1} by definition, and the SERs of the geothermal exergy and the tidal exergy are 4,900 seJ J^{-1} and 30,900 seJ J^{-1} respectively (Brown et al., 2016).

2.2.2 Secondary and tertiary exergy sources

Unit emergy values for the secondary and tertiary renewable fluxes were computed using the available energy derived from spatial coverages as outlined above. This method is a new approach to computing UEVs and as a result they differ from UEVs previously computed from global average data.

Wind UEV - The global average UEV for wind was calculated by dividing the global emergy baseline (GEB; 12.0 E+24 sej y^{-1}) by the wind exergy.

Rain UEV - The UEV of terrestrial rain was computed following the method of Odum (2000), where the GEB is divided by the exergy of terrestrial rainfall.

Actual Evapotranspiration (AET) UEV – The UEV of AET, following the method of Odum (2000), was assumed equal to that of rainfall

Runoff chemical potential UEV – The UEV of runoff chemical potential was computed assuming that AET and runoff is a split of rainfall. Thus, the emergy driving runoff is the portion that is not evapotranspired. The UEV was then computed by dividing the emergy by the total chemical potential of runoff.

Runoff geopotential UEV – The UEV of runoff geopotential exergy was computed in the same manner as runoff chemical potential where the emergy driving runoff (emergy of rainfall – emergy of AET) was divided by the sum of geopotential exergy in each cell of the coverage.

2.3 Emergy algebra for global empower map

Brown and Ulgiati (2016) proposed a new algebra for computing Aerial Empower Intensity (AEI) from renewable sources. This new method sums the tripartite and compares the total to the largest of the secondary and tertiary sources, taking the larger of these two values as the emergy input. The AEI of each cell in the global coverage was computed in this manner. The global empower coverage was developed by overlaying the coverages of each emergy source and using the algorithm from Brown and Ulgiati (2016) to compute total emergy input to each cell with a slight variation from the Brown and Ulgiati methodology. It was obvious with these spatial data that we could compute the chemical potential emergy of runoff within each cell based on the difference in concentration of TDS from one cell to the next. Thus once computed, emergy of runoff chemical potential could be added to the emergy of AET to yield a total water chemical potential emergy. The total water chemical potential emergy was compared with wind emergy and runoff geopotential emergy to determine the max emergy on a cell by cell basis.

2.4 Continental empower

Primary, secondary and tertiary empower coverages were "clipped" to terrestrial continental boundaries and renewable empower computed for each continent using the max emergy algebra algorithm (Brown and Ulgiati, 2016). The method of computing the Max Empower for continents was first, to sum empower of all 1 arc degree cells within each clipped coverage (solar, geothermal and tidal exergy) to result in the sum of the primary sources. Second, to sum the secondary and tertiary empower across all 1 arc degree cells for their respective coverages

[a] The term solar equivalence ratio was established by Brown et al. (2016) recognizing that tidal and geothermal exergy are not derived from solar exergy, but are independent renewable sources to the geobiosphere. Both tidal and geothermal exergy as well as solar exergy are expressed in solar equivalent joules, abbreviated (seJ).

Table 3 Renewable exergy, SERs, global UEVs and emergy of the geobiosphere, with comparison of UEVs from Brown and Ulgiati (2016).

Item	Exergy[a.] (this study)	Exergy (Brown and Ulgiati, 2016)	Average Global SER or UEV (this study) [b.]	SER or UEV (Brown and Ulgiati, 2016)	Solar Emergy (this study)
	($J\ yr^{-1}$)		($seJ\ J^{-1}$; $sej\ J^{-1}$)		($seJ\ J^{-1}$; $sej\ yr^{-1}$)
Primary Sources					
Solar	3.7 E+24	3.7 E+24	1	same	3.7 E+24
Geothermal	9.5 E+20	9.5 E+20	4,900	same	4.7 E+24
Tide	1.2 E+20	1.1 E+20	30,900	same	3.6 E+24
TOTAL					12.0 E+24
Secondary & Tertiary Sources					
Wind, kinetic Energy	2.3 E+22	1.5 E+22	520	800	12.0 E+24
Terrestrial Rain, chemical potential	5.1 E+20	5.3 E+20	23,600	7,000	12.0 E+24
AET, chemical potential	3.5 E+20	NA [c.]	23,600	7,000	8.1 E+24
Runoff, chemical potential	1.8 E+20	1.8 E+20	20,900	21,300	3.9 E+24
Runoff, geopotential	1.2 E+21	2.9 E+20	3,220	12,800	3.9 E+24

a. Exergy fluxes were computed in this study using sources and methods outlined above.

b. Obtained by dividing the emergy in the last column by the exergy in column 2.

c. Not computed by Brown and Ulgiati (2016).

(wind, AET, runoff chem., water chem., runoff geo.) and take the maximum value. Finally to compare the primary sources total with the largest of the secondary and tertiary sources and use the larger of the two values. The method used above for the geobiosphere applied the max emergy algebra algorithm to *each cell,* while in the continental analysis, the algorithm was applied to each of the 7 *continent polygons* rather than each cell.

3 Results and discussion

3.1 Global exergy data

Figure 1 shows global coverages of renewable exergy inputs to the geobiosphere, and Table 3 lists the total exergy, UEVs and empower for each of the renewable sources. Also shown in Table 3 are the SERs (Brown et al., 2016) and UEVs from and Brown and Ulgiati (2016) for comparison with this study.

The exergy fluxes (Figure 1, Table 3) of the tripartite (solar, tidal and geothermal sources) are very similar to those in Brown et al. (2016) and since the SERs from that study were used in this study, the GEB that results is identical. There are some notable differences in the secondary and tertiary sources that result from differences in coefficients, data sources and most importantly the finer resolution of the analysis. The difference in total wind energy (2.3 E+22 J yr^{-1} compared to 1.5 E+22 J yr^{-1}) between this study and that of Brown and Ulgiati (2016) is almost entirely the result of a difference in the surface roughness exponent in land surface. While Brown and Ulgiati used 0.25 as average land surface roughness exponent and assigned it globally, in this study we assigned the surface roughness exponent within each cell based on the land cover data (see Table 2). Just for comparison, the average surface roughness exponent calculated for all 1 arc degree cells in this study was 0.28. Because of this difference, the geostrophic wind velocity over land is faster which causes higher total wind energy absorbed on land (2.3 E+22 J yr^{-1}) than that computed by Brown and Ulgiati (1.5 E+22 J yr^{-1}).

Interestingly, the chemical potential exergy of terrestrial rainfall was similar between both studies. Brown and Ulgiati (2016) using an average annual terrestrial rainfall of 1.13 E+05 km^3 (1.13 E+20 g) computed total terrestrial exergy of 5.3 E+20 J yr^{-1}, while in this study terrestrial rainfall derived from the WorldClim data

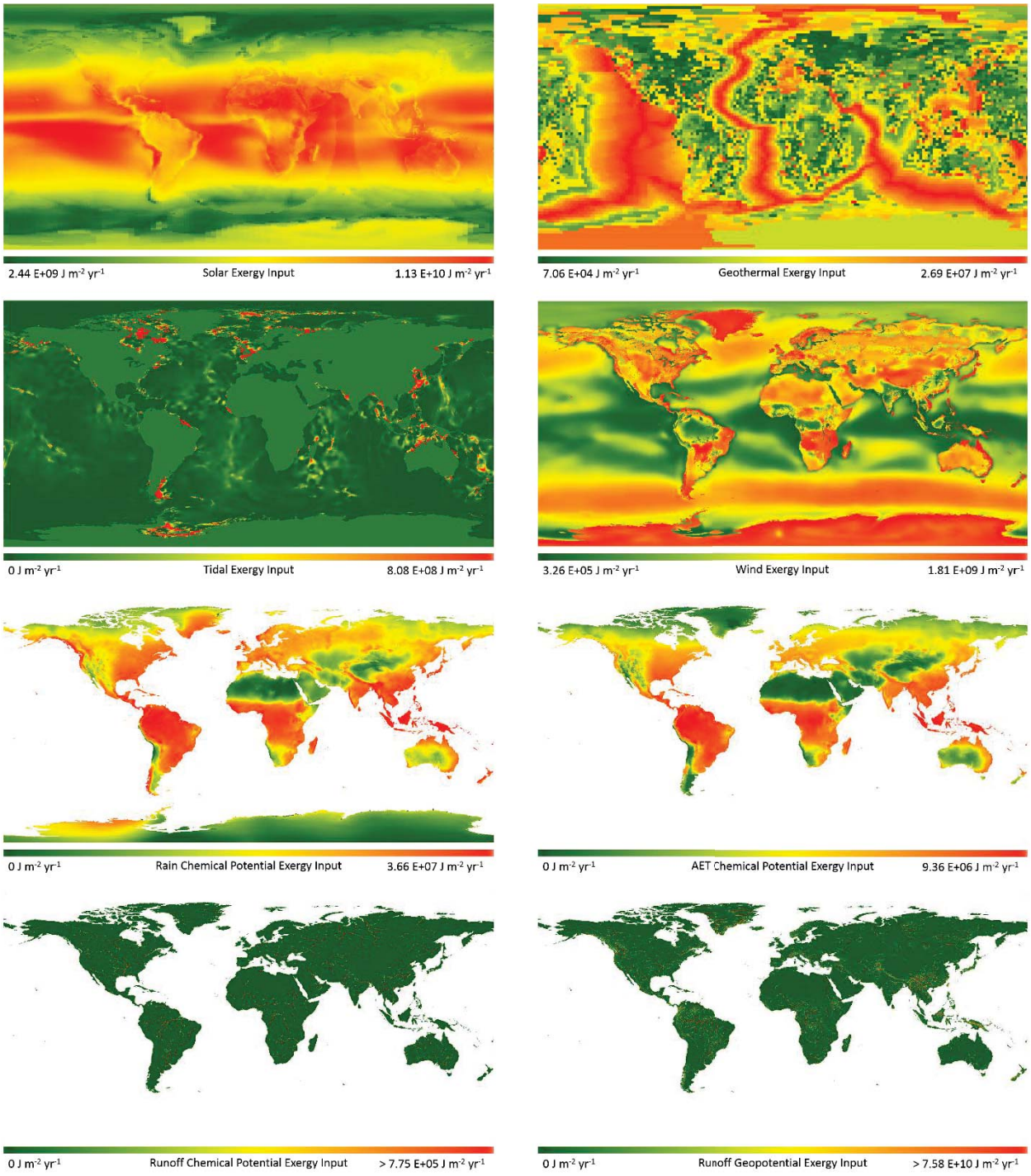

Fig. 1 Coverages of global renewable exergy inputs by source. From top left, solar, geothermal, tidal, wind, AET chemical potential, runoff chemical potential, total water chemical potential (sum of AET and runoff chemical potential), and runoff geopotential exergy.

(Fick and Hijmans, 2017) equaled 5.1 E+20 J yr^{-1}.

With the available data sets we were able to compute total global terrestrial actual evapotranspiration (AET), something that Brown and Ulgiati (2016) were not able to do. Using the Gibbs energy of rainfall, the chemical exergy of AET was computed as 3.5 E+20 J yr^{-1}.

Runoff was computed for each cell of the global coverage by subtracting AET from rainfall. This represents a significant difference between Brown and Ulgiati (2016) and the current work. In the former study they used an average global river discharge of 3.73 E+04 km^3 y^{-1} (Dai et al., 2009), while in the current study runoff was computed at a much finer resolution, that of 10 arc minute cells, and when summed totaled 3.74 E+04 km^3 y^{-1}. However, in this study, the total runoff was not used to compute either the chemical or geopotential exergy. Instead, we computed incremental exergy (from one cell to the next downstream cell until the flow reaches an estuary) across the entire global coverage. Total global chemical and geopotential exergy was then computed as the sum of the exergy absorbed in each 10 arc minute cell. Global chemical exergy of runoff computed in this way equaled 1.8 E+20 J yr^{-1} and global geopotential exergy was 1.2 E+21 J yr^{-1}. Chemical exergy of runoff computed in this way was very close to that of the Brown and Ulgiati study (1.8 E+20 J yr^{-1}) and the global geopotential exergy computed in this study was about 4x that computed in the Brown and Ulgiati study.

3.2 Global empower coverages

The result of global renewable emergy inputs expressed as Aerial Empower Intensity (AEI: sej m^{-2} yr^{-1}) is shown in Figure 2. Note that the scale of AEI for each coverage is different. The emergy of each renewable source is listed in Table 3. AET and Runoff chemical potential emergy are summed to equal the *total water chemical potential* in each cell. This represents the total renewable emergy from both transpiration by vegetation and the chemical potential of the runoff water. The impact of terrestrial albedo is evident in the solar empower coverage where the outline is visible against the large absorption of solar energy by the oceans. Also very evident is the spatial distribution of geothermal emergy, the largest concentrations are in the deep oceans along the mid ocean ridges. Tidal emergy is concentrated in coastal areas where coastlines and ocean bottom concentrate the tidal wave increasing the geopotential of the water in these restricted locations. Two phenomena dictate the empower distribution of wind emergy. The first is global geostrophic winds which are largest in the southern hemisphere along the 40^{th} meridian (also known as the "roaring 40's) where only a minor amount of land interrupt the continuous circulation of wind. The second is the "roughness" of terrestrial lands, where the highest absorption of wind is found in areas with the highest friction due to vegetation and topographic roughness.

Shown in Figure 3 is a coverage of the global renewable AEI that results from application of the max emergy algebra algorithm (Brown and Ulgiati, 2016) and dividing the maximum emergy by area of each cell. The largest AEI is in areas of tidal concentration in the northern part of North America, the British Isles, Northern Europe, and along the western coasts of Asia. Several areas along the eastern coast of South America also have high tidal AEI. Areas of high rainfall, which leads to high AEI and runoff chemical potential associated with total water chemical potential are visible throughout the tropical belt both north and south of the equator.

Summing the empower in each cell of the global coverage yields a total global empower of 16.2 E24 sej yr^{-1}, which is about 35% higher than the GEB (12.0 E24 sej yr^{-1}). This is a consequence of the Modifiable Areal Unit Problem [(MAUP); Gehlke and Biehl, 1934]. We will return to this issue in a later section of this paper.

3.3 Global unit emergy values for renewable empower

UEVs computed in this section are average global values. In a later section we compute UEVs for continents and major river basins.

Shown in column 4 of Table 3 are the global UEVs computed using the spatial data. There were several differences in UEVs between the current study and the Brown and Ulgiati (2016) study (column 5 in Table 3). While UEVs assigned to the tripartite were the same as those used in the previous work, the methods and data that were used for the secondary and tertiary renewable sources resulted in very different UEVs between the two approaches.

Because of the difference in exergy of wind (the current study was significantly higher), the UEV computed for global wind (520 sej J^{-1}) was about 65% of that in the Brown Ulgiati study (800 sej J^{-1}).

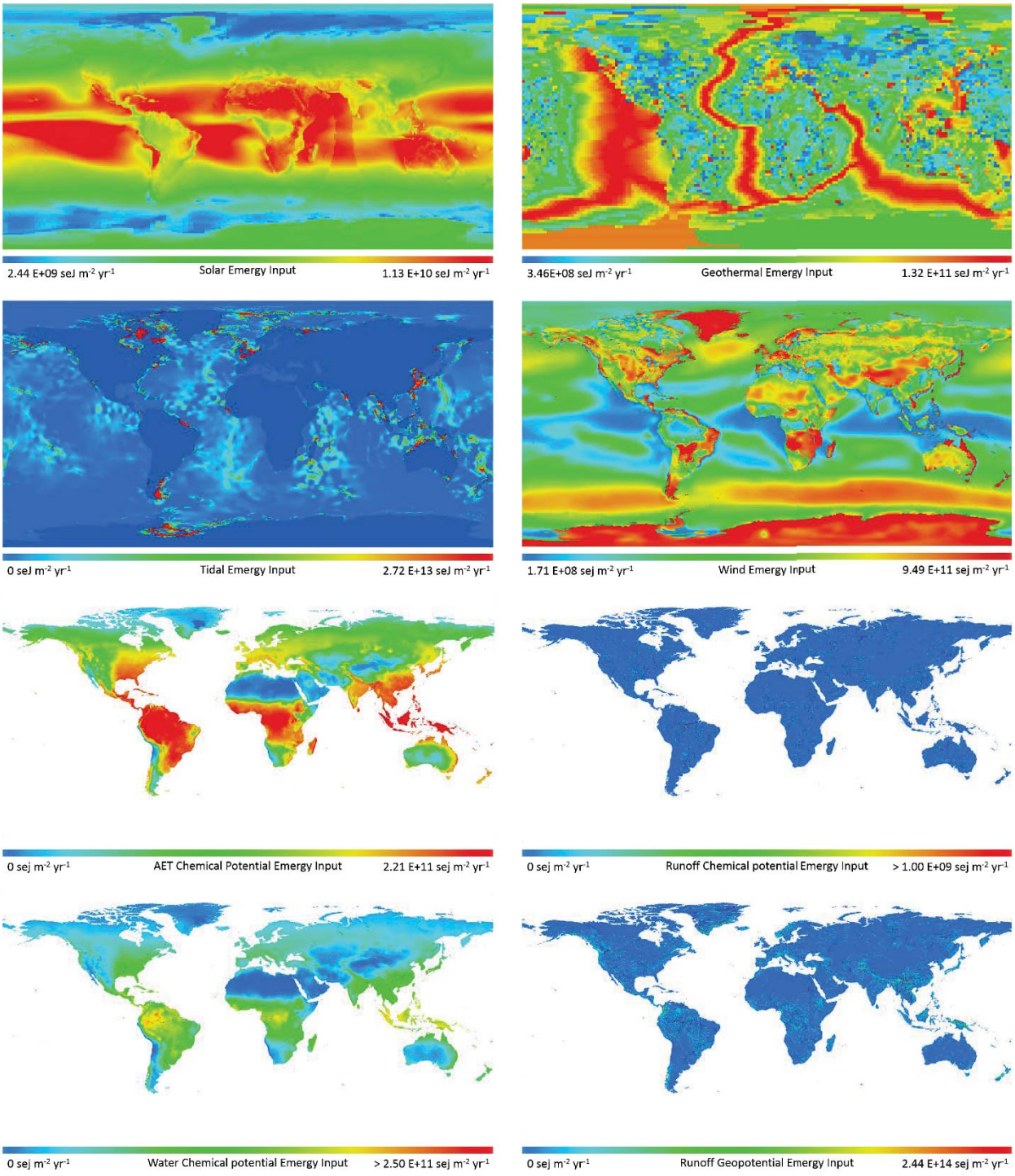

Fig. 2 Coverages of global renewable emergy inputs by source. From top left: Solar, geothermal, tidal, wind, AET chemical potential, runoff chemical potential, total water chemical potential (sum of AET and runoff chemical potential), and runoff geopotential emergy.

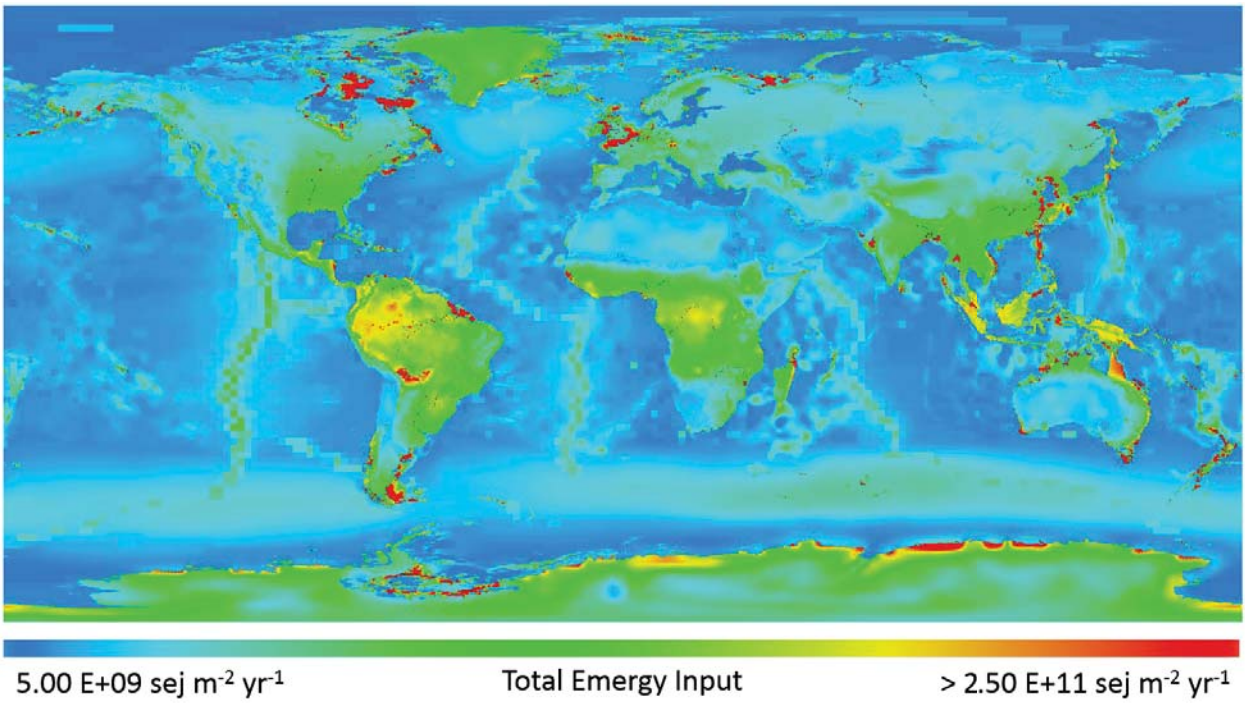

Fig. 3 Global aerial empower intensity (AEI) of renewable emergy.

A major difference between the two studies is the assumption of driving emergy of terrestrial rainfall. In the Brown and Ulgiati study, they used a matrix technique to assign only a portion of the GEB to terrestrial rainfall under the assumption that rain on land and rain on the ocean was a split of total global rainfall. In the current study, we assigned the entire GEB to terrestrial rainfall following the method of Odum (2000). The combination of slightly lower chemical potential of rainfall and the much larger driving emergy, resulted in the UEV of terrestrial rain of 23,500 sej J^{-1} compared to 7,000 sej J^{-1} in the Brown and Ulgiati study; a greater than 3 fold difference. The UEV computed for the rain chemical potential energy was also applied to the AET chemical potential energy.

Since AET and runoff are a split of rainfall (globally, about 30% of rainfall runs off the land, but varies considerably depending on many local factors, not the least of which is AET), the emergy assigned to runoff is that portion of the GEB that is not assigned to AET. The emergy of AET was spatially computed as 8.1 E+24 sej yr^{-1}, therefore the emergy assigned to runoff was 3.9 E+24 sej yr^{-1} (12.0 E24 – 8.1 E+24 = 3.9 E+24). The UEV for chemical potential of runoff that results (20,900 sej J^{-1}), was computed by dividing the driving emergy by the exergy of runoff chemical potential (3.9 E+24 sej yr^{-1} / 1.8 E+20 J yr^{-1}= 20,900 sej J^{-1}).

Unlike the Brown and Ulgiati (2016) study where the UEV of runoff was higher than that of rainfall, in the current study the UEV of rain chemical potential was higher than the UEV of runoff chemical potential, suggesting that the pure water of rainfall is of a higher quality than the runoff water with higher TDS.

Because of the method of computing geopotential exergy of runoff, the exergy spatially computed in this study was about 4× higher than that computed in Brown and Ulgiati (2016) In addition in this study we assumed that the emergy driving runoff was a split of the total emergy (rainfall emergy – AET emergy). The combination of these two differences resulted in a global runoff geopotential UEV of 3,220 sej J^{-1}, a value about 1/4 that of the Brown Ulgiati study.

Table 4 Empower inputs from primary, secondary and tertiary sources to continents.

Continent	Solar	Geothermal	Tidal	Wind	Rain Chem.	AET Chem.	Runoff Chem.	Water Chem. [a.]	Runoff Geo.	MAX Empower [b.]
	(E22 seJ yr^{-1})			(E22 sej yr^{-1})						
Oceania	7.6	5.9	1.1	51.6	63.7	43.3	17.7	61.1	12.5	61.1
Antartica	6.1	9.6	0.7	122.1	20.8	0.0	–	0.0	–	122.1
Europe	10.8	13.8	2.3	79.6	132.7	97.0	34.3	131.3	19.1	131.3
North America	14.2	18.0	3.8	112.6	182.3	119.7	55.1	174.8	30.5	174.8
Africa	27.6	20.2	0.5	108.5	221.0	175.1	70.0	245.1	155.0	245.1
Asia	23.8	21.8	3.1	110.3	265.9	173.6	84.4	258.0	48.7	258.0
South America	14.1	11.8	0.6	67.8	304.4	204.1	124.1	328.2	101.4	328.2
Ocean [c.]	268.7	365.3	347.5	547.5	9.3	–	–	–	–	–
Total	373.0	466.5	359.5	1200.0	1200.0	1198.5	812.9	385.6	367.2	1320.6

a. Water Chemical emergy is the sum of chemical potential emergy of AET and runoff (does not always equal due to rounding).

b. Max Empower is the maximum renewable emergy input based on the max emergy algorithm (Brown and Ulgiati, 2016).

c. Ocean renewable emergy is not added since to do so would be double counting all ocean emergy.

3.4 Continental renewable empower

Table 4 lists the seven continents of Earth and the ocean and the empower associated with each of the renewable sources. The final column lists the Max Empower for each continent when the max algorithm was applied. It is important to note that the ocean is not added into the Max Empower column total. Since the ocean empower is included in all terrestrial emergy inputs to add it to the continents would double count the ocean emergy.

The total terrestrial empower of continents was 13.2 E24 sej yr^{-1}, a value about 10% higher than the GEB (we will come back to this difference in a section below). Recall that the total terrestrial empower of the geobiosphere was 16.2 E24 sej yr^{-1} when evaluated on a cell by cell basis. The difference between these two values points to a phenomena that has important methodological consequences, which we will return to below.

3.5 UEVs of continental and river basin renewable empower

Tables 5 and 6 list calculated UEVs of runoff chemical and geopotential potential exergy for continents and 20 largest global river basins. The continental data in Table 5 shows runoff chemical potential UEVs vary about 75% from a low 13,700 sej J^{-1} (Africa) to a high 24,000 sej J^{-1} (Oceania) with the weighted mean value of 20,500 sej J^{-1}. Continental runoff geopotential UEVs varied about 450% with lowest UEV for Africa (1,300 sej J^{-1}) and highest for Oceania (7,100 sej J^{-1}), and a global weighted mean value of 3,200 sej J^{-1}. In Table 6, because of the differences in elevation of the river basins the computed UEVs vary more than the continental UEVs. Runoff chemical potential UEVs vary from a low of 4,700 sej J^{-1} (Niger) to a high of 696,000 sej J^{-1} (Lake Chad), a difference of about 15,000%. Runoff geopotential UEVs vary from a low of 700 sej J^{-1} (Zambezi) to a high of 5,400 sej J^{-1} (Ganges) a difference of about 670%. We have computed UEVs for 254 derivative vector major river basins features developed by the World Resources Institute (WRIBASIN; Jenness et al., 2007a, 2007b), which are included in supplemental material to this manuscript.

The variation in UEVS for both continents and river basins is partly due to a phenomena known as the Modifiable Areal Unit Problem (MAUP), an interesting issue we will return to in a later section. Suffice it to say that while some of the differences are the result of differences in rainfall, AET, size and topography of continents and watersheds, some of the variance results from the MAUP.

Table 5 Unit emergy values computed for continents.

Continent	Emergy (E+24 sej y^{-1})			Exergy [b.] (E+18 J y^{-1})		UEVs [c.] (E+03 sej J^{-1})	
	Rain Chem. Pot.	AET Chem. Pot.	Runoff [a.]	Runoff Chem. Pot.	Runoff Geo. Pot.	Runoff Chem. Pot.	Runoff Geo. Pot.
Antarctica	0.21	–	–				
Oceania	0.64	0.43	0.20	8.48	28.41	24.0	7.2
Asia	2.66	1.74	0.92	40.35	270.29	22.9	3.4
North America	1.82	1.20	0.63	26.33	192.24	23.8	3.3
South America	3.04	2.04	1.00	59.32	242.21	16.9	4.1
Europe	1.33	0.97	0.36	16.41	120.12	21.8	3.0
Africa	2.21	1.75	0.46	33.47	345.05	13.7	1.3
Global total	11.91	8.13	3.78	184.36	1198.31	20.5	3.2

a. Emergy of runoff equal to emergy of rainfall minus emergy of AET (column 3 – column 4).

b. Exergy is computed from spatial coverages.

c. UEV computed by dividing emergy by exergy.

Table 6 Unit Emergy values computed for 20 largest global river basins.

Basin	Area[a.] (E+06 km^2)	Emergy (E+21 sej yr^{-1})			Exergy[c.] (E+18 J yr^{-1})		UEVs [d.] (E+03 sej J^{-1})	
		Rain Chem. Pot.	AET Chem. Pot.	Runoff[b.]	Runoff Chem. Pot.	Runoff Geo. Pot.	Runoff Chem. Pot.	Runoff Geo. Pot.
Amazon	6.03	1440.5	921.3	519.2	29.6	126.9	17.5	4.1
Zaire	3.68	619.3	503.0	116.3	11.2	137.8	10.4	0.8
Mississippi	3.23	281.7	227.9	53.9	8.6	23.0	6.2	2.3
Ob	3.09	148.9	120.3	28.6	1.5	6.6	18.5	4.4
Nile	3.05	214.3	176.8	37.4	5.2	70.0	7.2	0.5
Parana	2.56	331.2	271.1	60.1	8.2	33.8	7.4	1.8
Lena	2.42	100.4	86.0	14.4	0.1	20.3	130.0	0.7
Amur	2.22	124.9	105.9	18.9	1.6	21.2	11.9	0.9
Niger	2.19	157.3	124.4	32.9	7.0	36.9	4.7	0.9
Yenisei	1.92	96.2	75.3	20.9	2.3	21.0	9.1	1.0
Yangtze	1.70	199.0	153.4	45.6	0.3	79.5	147.8	0.6
Ganges-Brahmaputra	1.66	222.8	135.2	87.7	6.8	16.2	12.9	5.4
Mackenzie	1.54	73.7	58.6	15.1	0.6	12.5	23.7	1.2
Lake Chad	1.50	91.0	77.7	13.3	0.0	4.7	696.0	2.8
Volga	1.40	85.2	67.6	17.6	0.2	12.0	106.8	1.5
Zambezi	1.38	140.8	117.8	23.0	2.8	34.3	8.2	0.7
Saskatchewan-Nelson	1.14	62.5	51.1	11.4	0.1	2.1	99.2	5.4
St. Lawrence	1.06	106.3	73.9	32.4	1.6	6.9	19.9	4.7
Murray-Darling	1.04	56.3	47.9	8.4	0.1	3.5	131.8	2.4
Indus	1.03	41.9	34.6	7.3	1.3	8.6	5.7	0.9

a. Area data are calculated from this study as sum of cell area within each basin.

b. Emergy of runoff equal to emergy of rainfall minus emergy of AET (column 3 – column 4).

c. Exergy is computed from spatial coverages.

d. UEV computed by dividing emergy by exergy.

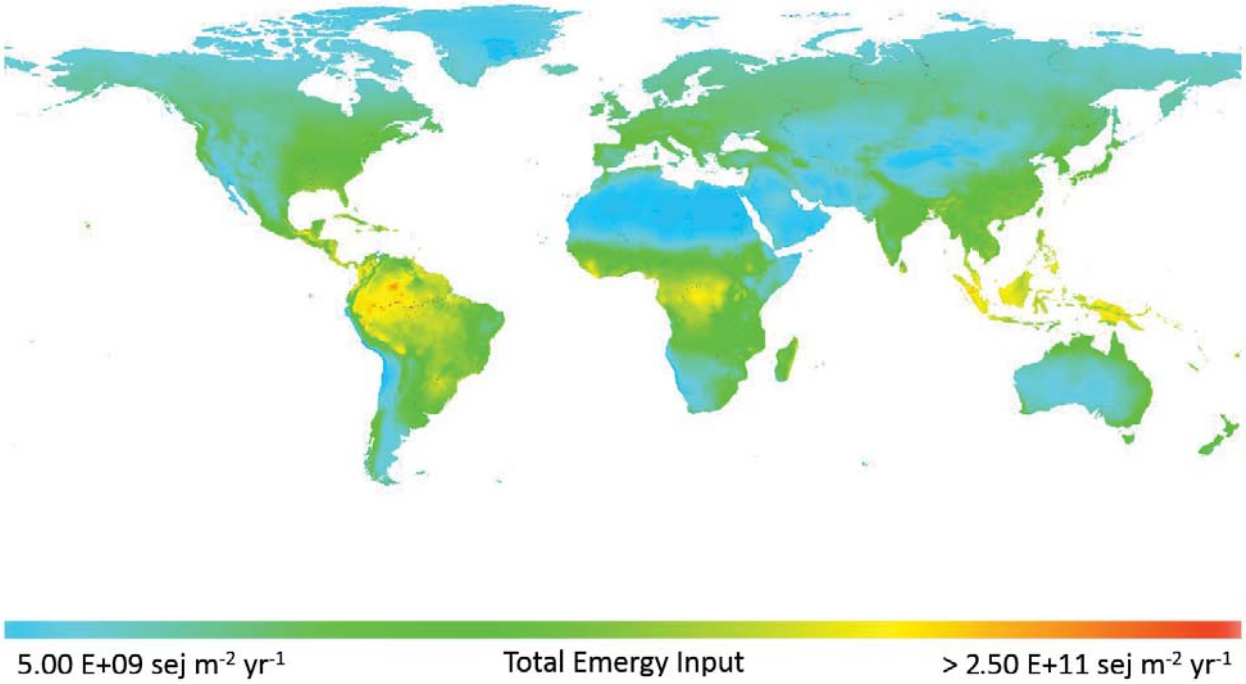

Fig. 4 Global aerial empower intensity (AEI) of terrestrial renewable emergy.

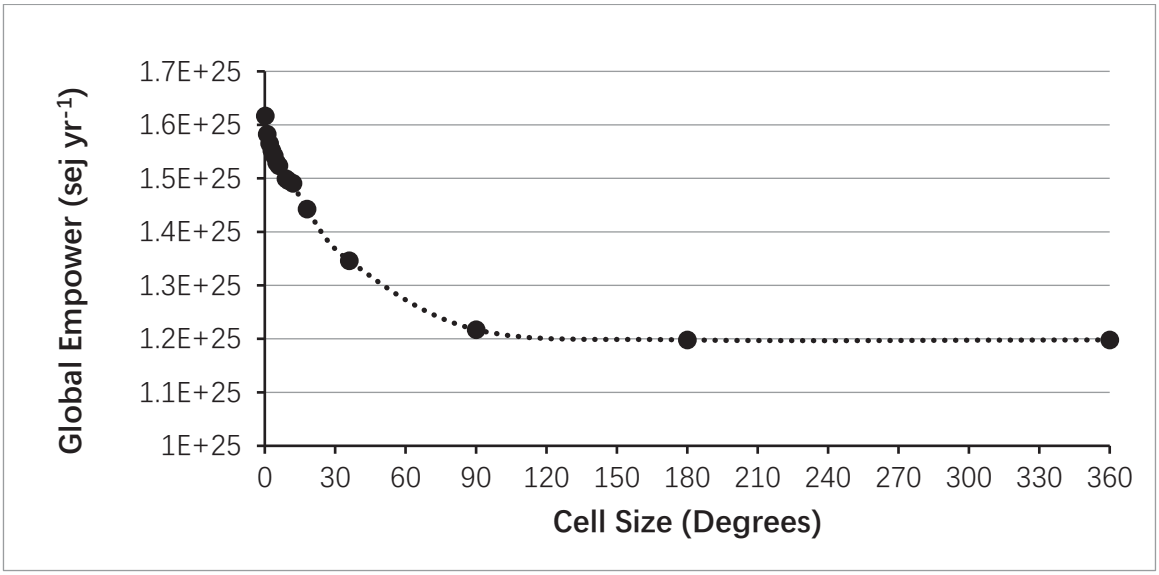

Fig. 5 Graph showing the trend of global total empower vs. resolution (in degrees). The change in total empower is the result of what is known as the Modifiable Areal Unit Problem where higher resolution data yields higher total empower when calculated based on the max emergy algebra algorithm.

3.6 Global double counting

Figure 4 shows the global AEI with the oceans removed. Since the ocean represents that portion of the geobiosphere that contributes emergy to the terrestrial system, when summing the emergy in each cell that results from the application of the max emergy algebra algorithm, including the ocean would double count 71% of the GEB. Another way of saying this is that the computation of wind, rain, and therefore AET, and runoff is done

assuming that the entire GEB is necessary to produce them. Therefore if the ocean were added in, the portion of the GEB that is spatially assigned to the ocean (approximately 71%) would be double counted.

Summing the renewable emergy in each terrestrial cell that results from the application of the max emergy algebra algorithm and using the 1 arc degree cell size resulted in total global empower of 16.2 E24 sej yr^{-1}, a value that is 35% larger than the GEB[b]. Interestingly, depending on the size of cells (raster cell size), the total global empower varies from 16.2 E24 sej yr^{-1} to 12.0 E24 sej yr^{-1} (Figure 5). As the cell size increases until it reaches 1 cell (360°: the entire globe) global empower decreases until it reaches the value of the GEB (12.0 E24 sej yr^{-1}), the result of a well known phenomena in spatial analysis known as the Modifiable Areal Unit Problem (MAUP) (first identified by Gehlke and Biehl, 1934). While there are two issues of concern within the MAUP, the one that produces the aforementioned effects is the "scale effect", which in essence leads to variation in numerical results due to the number of areal units used in the analysis of a given area (Openshaw and Taylor, 1979). When areal units are aggregated into fewer, larger units for statistical analysis, values associated with the variation of the data decrease.

Obviously this has interesting implications when spatial data are aggregated into smaller units like continents, river basins and countries. When computing total renewable emergy input to geobiosphere as a single system, the largest input is the sum of the tripartite, which results in a biosphere total empower of 12.0 E24 sej yr^{-1}. But when computing in smaller subsections, the source of largest input varies causing differences in the overall total. Thus clipping the biosphere into continents and applying max empower to each continental polygon, yielded total global empower of 13.2 E24 sej yr^{-1}. Therefore, higher resolution results in higher emergy input as shown in Figure 5. This issue also occurs in the National Environmental Accounting Database (NEAD) (Sweeney et al., 2006). When summing all the terrestrial renewable inputs based on the max emergy algorithm, the total is 23.8E+24 sej yr^{-1} (GEB; 15.2E+24 sej yr^{-1}).

3.7 Limitations

This study assumes an annual steady state environment which means it does not take a changing climate into consideration. We have used average annual data based on the availability of the spatial data record. In some cases the record is 22 year in length (solar), of variable length (geothermal), 30 years (rainfall), and 10 years (wind). AET has no annual record, but is based on a modeled annual average using 50 years of climate input drivers. In other words there is no annual variation implicit in these data.

Since no raster can perfectly reflect reality, there are always distortions on the edges of spatial units, especially on the coastlines. This problem can be minimized to some extent by applying higher resolution datasets, but not all data are available in high resolution in every location (and of course very high resolution data analysis at the global scale comes with a very large cost in computational time). A general principle in spatial analysis is that the working resolution of combinations of spatial data sets of different resolution is determined by the data with the coarsest resolution. The working resolution in this study was 1 arc degree, which represents a cell size of 111.3 km on a side (12,390 km^2) at the equator. This coarseness means that at the boundaries of spatial units (coastlines, boundaries of river basins) there is the potential for aggregation error.

Finally, another limitation is from the UEVs used in this study. We have shown that UEVs can vary based on processes and/or location even for the same type of energy (runoff chemical and geopotential UEVs). While it may be possible, to date we have not computed spatially explicit UEVs for solar energy, rainfall, geothermal tidal or wind inputs[c]. This study has used global average UEVs, but has computed spatially explicit UEVs for the available energy from runoff chemical and geopotential sources. The more we work with these spatial data sets the stronger we feel that spatially explicit UEVs are the next step in evaluating global renewable empower.

[b] We have removed oceans from this summation since to add the ocean data would double count it because the total GEB (which includes the ocean emergy) is driving the terrestrial rain and wind input.

[c] It should be noted that Brown and Ulgiati (2016) computed different terrestrial and oceanic UEVs for wind and rainfall. In this study however, we used global averages instead of these spatially explicit ones.

4 Conclusion

This study has developed global coverages of individual energy sources and a total renewable empower map in 1 arc degree resolution using the spatial data derived from the latest satellite-based models. These coverages facilitate analysis of renewable sources at different spatial resolutions. The important findings of the study are the fact that rain water has higher quality than the stream water, and the fact that even though there have been efforts to eliminate the double counting (using the Max emergy algorithm), the tendency to double count emergy inputs increases with increasing spatial resolution.

The spatial data sets allowed us to compute spatially explicit UEVs for the available energy in runoff chemical and geopotential based on a split of the emergy in rainfall between AET and runoff. By computing available energy on a cell by cell basis it was possible to develop a spatial coverage for chemical and geopotential exergy. The emergy of runoff was taken as the emergy of rainfall minus AET and when divided by exergy in chemical and geopotential of runoff yielded unique UEVs for continents and 20 of the worlds largest river basins (Actually the supplemental material contains unique UEVs for about 254 global river basins). Continental runoff chemical potential UEVs were shown to vary about 75% from a low 13,700 sej J^{-1} (Africa) to a high 24,000 sej J^{-1} (Oceania) with the weighted mean value of 20,500 sej J^{-1}. Continental runoff geopotential UEVs varied about 450% with lowest UEV for Africa (1,300 sej J^{-1}) and highest for Oceania (7,100 sej J^{-1}), and a global weighted mean value of 3,200 sej J^{-1}.

Finally, we explored the implications of the Modifiable Areal Unit Problem (MAUP) on the evaluation of renewable empower. Since renewable emergy inputs are, for the most part, spatial in character, the evaluation of regions of the geobiosphere are inherently vulnerable to issues of scale and aggregation which will lead to the appearance of double counting and a source of statistical bias. The choice of district or regional boundaries and the real-world patterns in the renewable emergy flows being evaluated contribute to MAUP issues at these smaller scales. While much has been written about the MAUP and suggestions made to counter its effects, there is general agreement that it is fundamentally an intractable unsolvable issue.

As was shown in the continental analysis when the "cell size" was small (i.e., 1 arc degree) and the max emergy algorithm was applied to each cell individually and then summed for the continent, the global empower was 16.2 E24 sej yr^{-1}, While when the max emergy algorithm was applied to each continent as a whole, the global terrestrial total was 13.2 E24 sej yr^{-1} an increase of 10% over the GEB (12.0 E24 sej yr^{-1}). Considering this outcome we suggest that evaluations that employ the max emergy algebra and GIS be done at the coarse scale of the regional boundary, rather than on a cell by cell basis. In other words summing input emergy within regions, then applying the max emergy algorithm as opposed to computing max emergy for each cell. This obviously still results in some error (10% at continental level) but is much better that the 35% error when the cell by cell method is applied.

5 Supplement data

Supplement data includes ASCII files of Global AEI, coverages of Solar, Tidal, Geothermal, Tripartite, Wind, Rain chemical potential, AET chemical potential, Runoff chemical potential, Water chemical potential, and Runoff geopotential. All coverages are in 1 arc degree resolution with the projection of WGS_1984. The Supplement data also includes unique UEVs for about 254 global river basins.

References

Brandt-Williams, S. and Brown, M.T. (2011), *Renewable emergy in earth's biomes,* Emergy Synthesis 6 Theory Application of Emergy Methodology Proceedings from 6th Biennial Emergy Conference 93-104.

Brown, M.T., Campbell, D.E., De Vilbiss, C., and Ulgiati, S. (2016), The geobiosphere emergy baseline: A synthesis, *Ecological Modelling*, **339**, 92-95.

Brown, M.T. and Ulgiati, S. (2016), Emergy assessment of global renewable sources, *Ecological Modelling*, **339**, 148-156.
Chandler, W., Whitlock, C., and Jr, P.S. (2005), *Determining Wind Resources as a Function of Surface Roughness and Height from Nasa Global Assimilation Analysis*, Proceedings of International Solar Energy Society (ISES) 2005 Sol. World Congress, Orlando, Florida.
Cook, G. and Dickerson, R.H. (1995), Understanding the chemical potential, *American Journal of Physics*, **63**, 737-742.
Dai, A., Qian, T., Trenberth, K.E., and Milliman, J.D. (2009), Changes in continental freshwater discharge from 1948 to 2004, *Journal of Climate*, **22**, 2773-2792.
Davies, J.H. (2013), Global map of solid Earth surface heat flow, *Geochemistry, Geophys Geosystems*, **14**, 4608-4622.
Egbert, G.D. and Ray, R.D. (2001), Estimates of M2 tidal energy dissipation from TOPEX/Poseidon altimeter data, *Journal of Geophysical Research*, **106**, 22, 422-475, 502.
Egbert, G.D. and Ray, R.D. (2000), Significant dissipation of tidal energy in the deep ocean inferred from satellite altimeter data, *Nature* **405**, 775-778.
Fick, S.E. and Hijmans, R.J. (2017), WorldClim 2: new 1-km spatial resolution climate surfaces for global land areas, *International Journal of Climatology,* **37**, 4302-4315.
Gehlke, C.E. and Biehl, K. (1934), Certain effects of grouping upon the size of the correlation coefficient in census tract material, *Journal of the American Statistical Association*, **29**, 169170.
Gibbs, R.J. (1967), Amazon river: environmental factors that control its dissolved and suspended load, *Science*, **156**, 1734-1737.
Jenness, J. Dooley, J. Aguilar-Manjarrez, J., and Riva, C. (2007a), *African Water Resource Database.* GIS-based tools for inland aquatic resource management. 1. Concepts and application case studies CIFA Technical Paper. No. 33, Part 1. Rome, FAO, 167p.
Job, G. and Herrmann, F. (2006), Chemical potential—a quantity in search of recognition, *European Journal of Physics*, **27**, 353-371.
Odum, H.T. (2000), *Emergy of Global Processes. Folio #2*: Handbook of Emergy Evaluation: A Compendium of Data for Emergy Computation Issued in a Series of Folios. Center for Environmental Policy, University of Florida, Gainesville, FL.
Openshaw, S. and Taylor, P.J. (1979), *A million or so correlation coefficients: three experiments on the modifiable areal unit problem*, In: N. Wrigley (Ed.). Statistical methods in the spatial sciences. London: Pion.
Sweeney, S., Cohen, M., King, D., and Brown, M.T. (2006), *Creation of a global emergy database for standardized national emergy synthesis*, Emergy Synthesis 4 Proceedings of 4th Biennial Emergy Research Conference, 23.1-23.
Trabucco, A. and Zomer, R.J. (2010), *Global soil water balance geospatial database*, CGIAR Consortium Spatial Information Public online, available from CGIAR-CSI GeoPortal, http://www.cgiar-csi.org